International Journal of Fatigue 161 (2022) 106915

Contents lists available at ScienceDirect

International Journal of Fatigue

journal homepage: www.elsevier.com/locate/ijfatigue

Strain energy density approach as fatigue assessment of Ti6Al4V specimens machined by WEDM single step technology

Simone Salamina [a,*], Daniele Crivelli [a], Luca Diviani [a], Filippo Berto [b], Seyed Mohammad Javad Razavi [b]

[a] Institute for Mechanical Engineering and Materials Technology, University of Applied Sciences and Arts of Southern Switzerland (SUPSI), Lugano, Switzerland
[b] Department of Mechanical and Industrial Engineering, Norwegian University of Science and Technology (NTNU), Trondheim, Norway

ARTICLE INFO

Keywords:
High cycle fatigue
Local approaches
Strain energy density
Ti6Al4V
WEDM

ABSTRACT

The present paper summarizes the results from force-controlled fatigue tests performed on Ti6Al4V specimens machined by wire electrical discharge machining (WEDM) single step technology. For this aim, blunt V-notched specimens with various notch root radii and un-notched "dog bone" specimens are considered. The fatigue behaviour of this alloy machined by WEDM single step technology is an extremely important issue but, despite this, the literature on this topic is very poor and the effect of geometrical discontinuities on the fatigue life of has still to be investigated.

Fatigue data, generated by testing a total number of 62 specimen, are re-analysed by means of the Strain Energy Density (SED) method, investigating the possibility to use this method following a numerical approach. Estimation of the critical radius is performed on the basis of finite element analysis to overcome the lack of knowledge of the material properties often related to the machining process.

Thanks to the SED method, it is possible to summarize in a single scatter-band all the collected fatigue data, independently of the specimen geometry. The proposed numerical approach is capable to reduce the scatter index compared to the actual procedure with modest extra effort, also solving the issue related to the geometry selection for the critical radius identification. The method is successfully validated by assessing the fatigue life of specimens with two notch geometries not considered during the critical radius identification.

1. Introduction

Ti6Al4V alloy is the most commonly utilized titanium alloy, with application in the most advanced engineering fields such as military, aerospace and naval application, thanks to its very good mechanical properties [1]. Fatigue cracks usually start from the surface of the components as they undergo the maximum stresses during exercises [2]. Machining is then a key factor to take into account when assessing fatigue life, because it is directly responsible for the surface integrity [23]. In this study, wire electrical discharge machining (WEDM) process is then considered, because it is a valid alternative for the machining of difficult-to-machine materials, such as Ti6Al4V (with conventional methods).

It is known that outdated or coarse EDM processing can reduce the fatigue strength of titanium alloy Ti6Al4V by as much as factors of 2–5 [4]. A suitable example is reported in the work of Janeček et al. [5] which compared rotating bending fatigue endurance of electro-polished specimen with aggressively eroded ones, demonstrating a severely reduced fatigue strength due to near surface tensile residual stresses, pre existing micro-cracks and high surface roughness all induced by EDM. In the latter, EDM process parameters were intentionally modified to obtain very rough surfaces, resulting in a reported surface roughness of $R_a = 11.6$ μm.

Nowadays, state-of-the-art EDM technology are able to reduce this detrimental effect thanks to the improvement of generator technologies and the use of multi-step technologies (one main cut followed by one or more trim cuts) [4,6]. In fact, studies from Klocke et al. [7] and Welling [8] demonstrate that WEDM specimens can show comparable or even better fatigue strength comparing to conventionally machined counterparts.

Nevertheless, WEDM single step technologies are still adopted in real life applications when cut speed is needed and rough surfaces are admissible. Despite this, up to this date quantitative data regarding fatigue and notch fatigue properties after WEDM main cut appear to be very poor or missing.

* Corresponding author.
E-mail address: simone.salamina@supsi.ch (S. Salamina).

https://doi.org/10.1016/j.ijfatigue.2022.106915
Received 10 December 2021; Received in revised form 11 March 2022; Accepted 9 April 2022
Available online 12 April 2022

Nomenclature

SED	Strain Energy Density
WEDM	Wire Electrical Discharge Machining
FEA	Finite Element Analysis
NSIF	Notch Stress Intensity Factor
e_1	Mode I geometric shape function
E	Young's modulus
I_1	Mode I function in SED expression for V-notches
k	Inverse slope of the linearized fatigue data
K_{IC}	Fracture toughness
K_1^V	Mode I NSIF
ΔK_{1A}	V-notched specimen NSIF-based fatigue strength
K_t	Notch stress concentration factor
K_f	Fatigue strength reduction factor
$K_{fV-Notch}$	Fatigue notch factor
q	Notch sensitivity
R_a	Arithmetical mean roughness
R_0	Control radius
r_0	Control radius center position
T_s	Stress based fatigue scatter index
T_w	SED based fatigue scatter index
W_c	Critical SED
$\overline{W}_1$	Mode I SED
$\Delta\overline{W}$	SED associated with the fatigue full range
$\Delta\overline{W}_u$	SED related to a nominal stress unitary load
$\Delta\overline{W}_{Exp}^{Smooth}$	SED associated with the experimental fatigue stress range (smooth specimen)
$\Delta\overline{W}_{Exp}^{Notched}$	SED associated with the experimental fatigue stress range (notched specimen)
$\overline{W}_{max}$	SED associated with the fatigue loading maximum stress
Greek	
2α	Notch opening angle
λ_1	Mode I William's eigenvalue
$\widetilde{\omega}_1$	Auxiliary parameter in Filippi's stress equations
υ	Poisson's ratio
ρ	Notch root radius
σ_{UTS}	Ultimate tensile strength of un-notched specimen
$\Delta\sigma_A$	Un-notched specimen fatigue strength
$\Delta\sigma_{Exp}^{Smooth}$	Experimental fatigue stress range (smooth specimen)
$\Delta\sigma_{Exp}^{Notched}$	Experimental fatigue stress range (notched specimen)
$\Delta\sigma_u$	Nominal unitary fatigue stress range (in the reduced section)
μ_1	Exponent in Filippi's stress equations

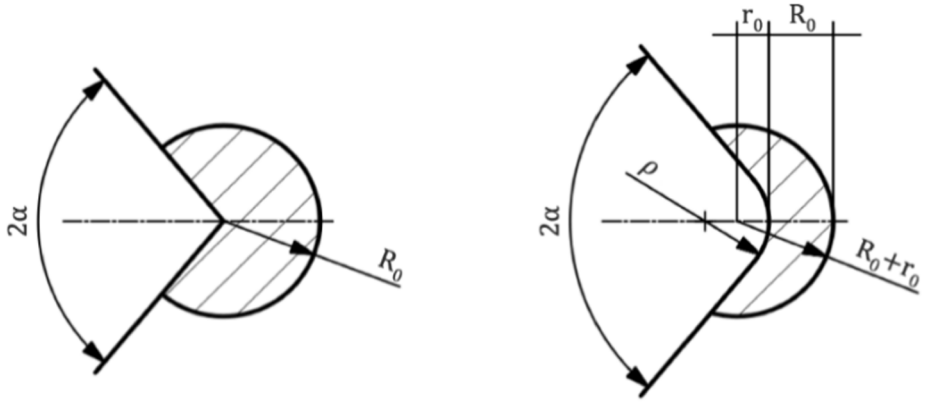

Fig. 1. Control volume geometry for sharp and blunt V-notches [16].

Table 1
Geometry features of each tested specimen (specimens written in bold tested during validation).

Specimen name	Notch root radius ρ [mm]	Notch opening angle 2α [°]
STR (smooth)	–	–
V90-R0.2	0.2	90
V90-R3	3	90
V90-R1	1	90
V90-R5	5	90

Real life components are characterized by geometrical discontinuities, often in the form of holes and notches, which act as crack starters leading to reduced fatigue life. Traditionally, to predict the failure of weakened components, generalized stress intensity factors are used, which are difficult to obtain and are geometry dependent. To assess the fatigue life of notched components it is useful to have a parameter which depends only on the material, such as the strain energy density criterion, and also to make use of numerical methods which can provide reliable results in a convenient time.

The volume-based SED criterion states that static failure occurs when the mean value of the strain energy density over a given, well defined, control volume (Fig. 1) reaches a critical value W_c [9]. Berto and Lazzarin [10] reported that these critical parameters, W_c and the control volume radius R_0, are only material-dependent. The method has been extensively and successfully used in the assessment of the tensile and fatigue behaviour of welded joints and different materials weakened by several notch geometries [11121314151617 18].

Looking back to the work of Lazzarin and Zambardi [9] the critical parameters of SED criterion can be obtained analytically directly from material properties including the ultimate tensile strength of un-notched specimen σ_{UTS}, the fracture toughness K_{IC}, the Young's modulus E, and the Poisson's ratio υ. The following expression reported from Beltrami's study [19] can be used to determine the critical strain energy density. Table 1.

$$W_c = \frac{\sigma_{UTS}^2}{2E} \tag{1}$$

In plane strain problems, the control volume is defined as a circular sector where the critical energy has to be evaluated, for V-Notches

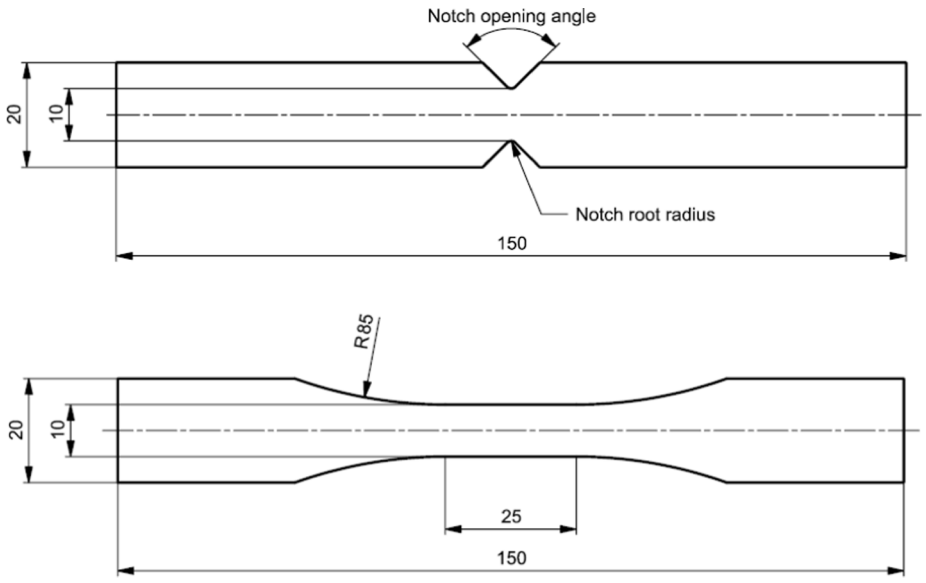

Fig. 2. Tested specimen geometry.

(Fig. 1) the critical radius can be expressed as follows [11]:

$$R_0 = \frac{(1+\upsilon)(5-8\upsilon)}{4\pi}\left(\frac{K_{IC}}{\sigma_{UTS}}\right)$$

The average strain energy density under to mode I loading can be computed by means of the following expression [11]:

$$\overline{W}_1 = \frac{e_1}{E}\left[\frac{K_1^V}{R_0^{1-\lambda_1}}\right]^2 \tag{3}$$

in which, e_1 (Equation (6)) is a geometrical shape function that depends on the notch opening angle 2α, K_1^V is the mode I notch stress intensity factor (NSIF), and λ_1 is the mode I Williams' series eigenvalue [20]. For blunt V-notches the position of the control volume is a function of the notch geometry, according to Fig. 1 [21], resulting in a shift of the control volume's center by a distance of r_0 defined as follows:

$$r_0 = \rho\frac{\pi-2\alpha}{2\pi-2\alpha} \tag{4}$$

Dealing with fatigue loading, the critical SED can be expressed as [9]:

$$\Delta\overline{W} = \frac{e_1}{E}\left[\frac{\Delta K_{1A}}{R_0^{1-\lambda_1}}\right]^2 \tag{5}$$

The shape function e_1 is directly dependent from the notch opening angle [9]:

$$e_1 = 4.809\cdot10^{-6}\cdot(2\alpha)^2 - 2.346\cdot10^{-3}\cdot(2\alpha) + 0.3400 \tag{6}$$

The control volume radius can be expressed as [11]:

$$R_0 = \left(\frac{\sqrt{2e_1}\,\Delta K_{1A}}{\Delta\sigma_A}\right)^{\frac{1}{1-\lambda_1}} \tag{7}$$

However, solving these analytical expressions is not an easy task. In fact, it requires material data that are not always available and dependent from the machining process [3], such as the fatigue strength of unnotched specimen, $\Delta\sigma_A$ (in order to quantify the influence of defects and surface roughness in the material, in absence of any global stress concentration effect) and the NSIF-based fatigue strength of notched specimens ΔK_{1A}.

In particular the computation of the NSIF for rounded notches [22], which requires the stress field ahead of the notch tip $(\sigma_\theta)_{\theta=0}$ (some explicit formulae can be found in [9] to analytically obtain it). The auxiliary parameters ($\widetilde{\omega}_1$, μ_1 *and* λ_1) are all function of the the notch opening angle [22].

$$K_1^V = \sqrt{2\pi}r^{1-\lambda_1}\frac{(\sigma_\theta)_{\theta=0}}{1+\widetilde{\omega}_1\left(\frac{r}{r_0}\right)^{\mu_1-\lambda_1}} \tag{8}$$

In aid of engineers come the FE codes, that enable the capability to easily compute the stress field in the vicinity of the notch or directly the strain energy density. Then, an estimation of the critical radius can be obtained equating the related critical SED values of two different specimen geometries [1723]. This approach was successfully adopted in the studies of Peron [1415] and Kusch et al. [16] for the failure assessment of notched specimen under mode I tensile loading, to overcome the lack of knowledge of the material properties such as the fracture toughness K_{IC}. Similar methodology was proposed in [1723] for SED analysis of fatigue behavior of notched components. In this work this kind of approach will be applied, with some modifications, on specimens machined by WEDM.

2. Methods

In this work the problem is faced following a combined experimental–numerical approach, a procedure similar to what was proposed by Razavi et al. [23], that will be adopted as reference. In fact, experimental data are used in combination with the unitary SED, $\Delta\overline{W}_u$, computed by FEA. In this way is possible to leave the control volume, therefore the critical radius R_0, as a variable. Fatigue data obtained by force controlled tests on three different geometries (1 smooth and 2 notched) are then transformed from S-N to SED-N data. For smooth specimen the transformation is simple, because SED is analytically calculated with Equation (9), derived from Equation (1), and not dependent from R_0.

$$\Delta\overline{W}_{Exp}^{Smooth} = \frac{\left(\Delta\sigma_{Exp}^{Smooth}\right)^2}{2E} \tag{9}$$

SED-N data are then linearized and statistically analysed for each R_0 value (R_0 resolution is set arbitrary at 0.01 mm). The optimal critical radius is defined as the one that shows the minimum scatter index T_s (T_w in terms of energy), which is the ratio between the stress amplitudes corresponding to 10% and 90% of survival probability, considering the whole dataset. Validation is performed testing two other notch geometries at different stress levels and verifying if they fall inside the previously computed scatter band.

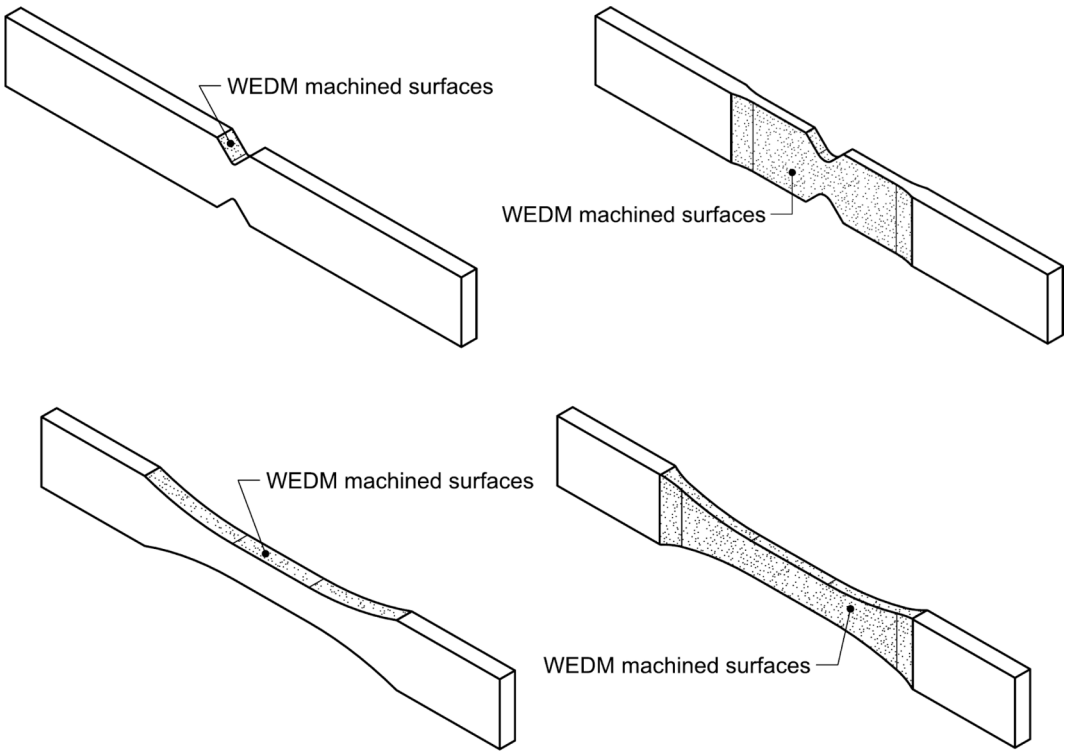

Fig. 3. Location of surfaces machined with defined WEDM process parameters, in the right side specimens with reduced thickness.

Table 2
Ti6Al4V properties for FEA.

Property	Value	Unit
Elastic Modulus	113,800	MPa
Poisson's ratio	0.34	–

For all the presented calculation, the fatigue load ratio R is assumed equal to 0. Therefore, the weighting factor c_w is equal to 1 [12], meaning no correction.

2.1. Test specimens

Three different specimen geometries are considered, one smooth specimen and two V-notched specimen (Fig. 2), to obtain the fatigue

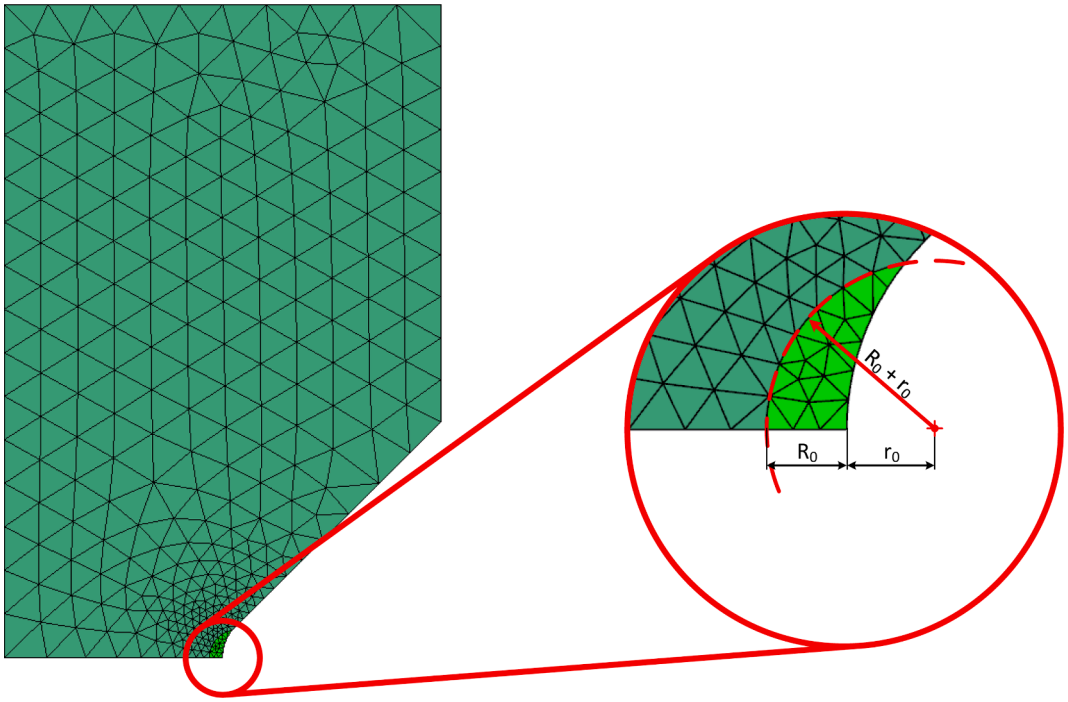

Fig. 4. Quarter notched specimen model, 2D mesh CTRIA(6) and control volume detail (optimal R_0, root radius 1 mm).

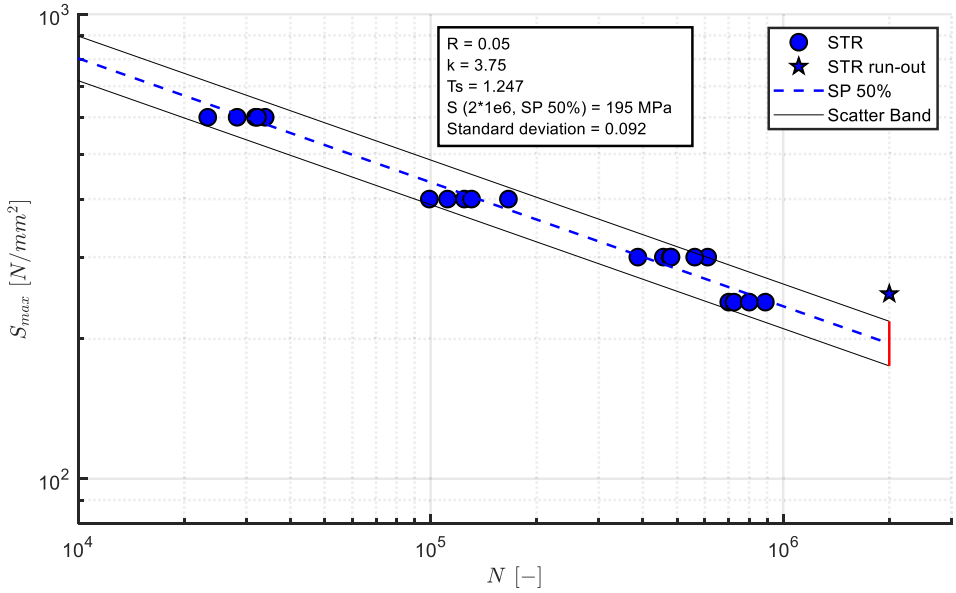

Fig. 5. Fatigue life of smooth (STR) specimens.

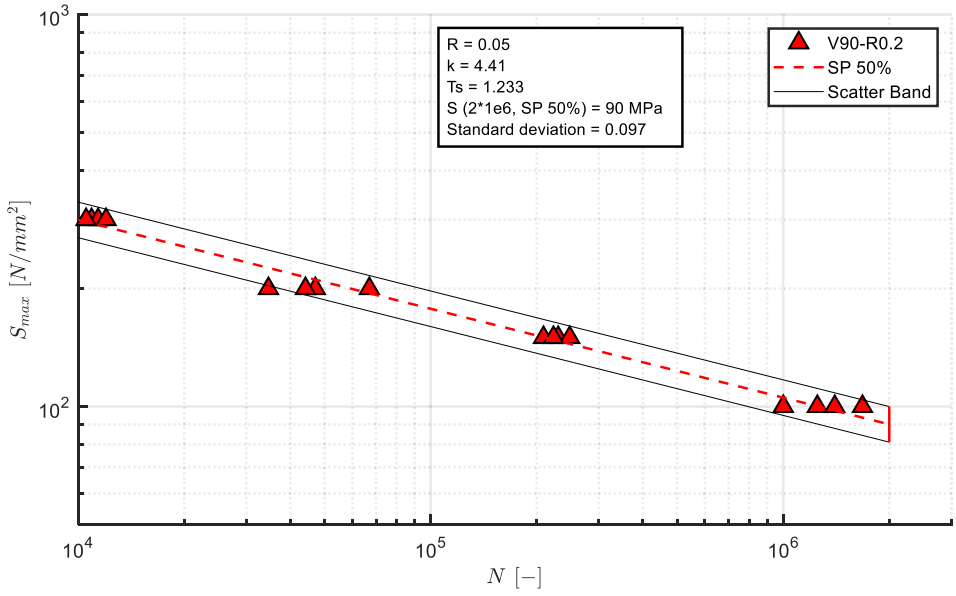

Fig. 6. Fatigue life of notched V90-R0.2 specimens.

data on which to evaluate the SED critical radius R_0 .

Then, two other notched specimen geometries are proposed in sight to validate the before mentioned critical radius.

2.2. Manufacturing and conditioning

Specimens are cut off by WEDM from annealed Ti6Al4V sheets of 5 mm thickness. The notch surfaces (where the fatigue cracks are most likely to initiate) are machined with the same WEDM process parameters (see Fig. 3). Some specimens are also machined through the thickness (in those cases specimen thickness was reduced to 3 mm) direction but no noticeable difference in fatigue life is observed after testing. No further treatment is performed on the specimens.

The Wire EDM machine used is a CUT X 350 (water based dielectric and 0.25 mm brass wire) from GF (GF Machining Solutions, Schaffausen, CH) and the process parameters are related to the standard titanium single step technology proposed by the machine manufacturer. The expected surface roughness was R_a 3 μm, measurement performed directly on the specimen showed an average roughness of R_a 3.4 μm.

Specific parameters used will not be related here, because the purpose of this study is not to investigate the impact of EDM processes parameters on the fatigue performance of the material, but rather to assess fatigue life by means of SED related to a standard EDM single step titanium technology.

2.3. Experimental testing

The experimental tests are performed on an MTS Landmark 100kN (MTS Systems Corporation, MN USA) servo-hydraulic universal testing device (±100 kN, ±75 mm) under load control. The load cell with ± 1% error at full scale has been used to measure the applied load. The specimen is fixed in the testing system by means of hydraulic grips. Suitable wedges are mounted in the grips according to the specimen thickness. All tests are carried out with alternating tensile stress (load

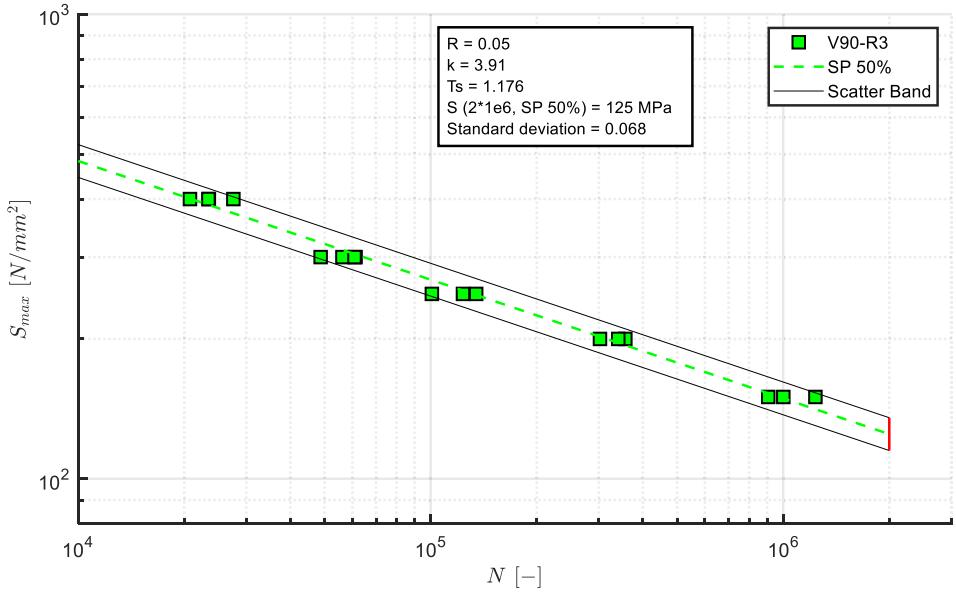

Fig. 7. Fatigue life of notched V90-R3 specimens.

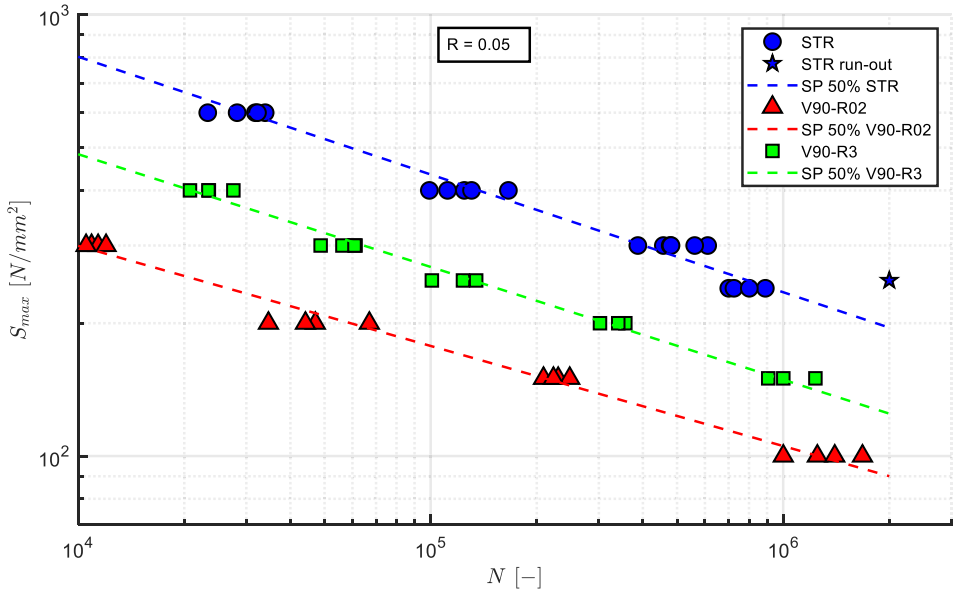

Fig. 8. Fatigue life of all R_0 optimization specimens.

ratio R = 0.05) with sine waveform (constant amplitude). Frequency of the test is set at 20 Hz for smooth specimen and at 30 Hz for the notched ones.

2.4. FEA and optimal R_0 computation

FE models are created with NX 12.0 (Siemens PLM Software, Plano, USA). Linear elastic plane stress simulations are performed using NASTRAN solver (MSC Software Corporation, Newport Beach, USA). The necessary material properties are obtained from the literature [24] and summarized in Table 2.

A quarter of specimen geometries are modelled with a 2D mesh with CTRIA(6) triangular parabolic elements, taking advantage of the double symmetry, with the appropriate boundary condition, to reduce model size and computational time. The control volumes, defined according to Fig. 1, with radii varying from 0.04 to 0.8 mm are modelled to evaluate the average value of the strain energy density vs R_0. The mesh size in the control volume is adapted to guarantee at least 16 elements in the control volume and precisely compute the SED value (a coarse mesh is in fact sufficient [25]), whereas the rest of the model is discretised using elements of size 1 mm, with a transition region to smoothly increase the element size (Fig. 4). The average value of the strain energy is calculated as the total strain energy, computed within the control radius, divided by the un-deformed volume, considering negligible displacement. Notched specimens used for the critical radius fit (V90-R0.2 and V90-R3) are computed applying to the model a nominal unitary load $\Delta\sigma_u$ equivalent to a nominal stress of 1 MPa in the reduced section. Thanks to this, it is possible to obtain a "unitary value" of the SED (defined as $\Delta\overline{W}_u$) vs R_0 and, taking advantage of the linear elastic hypothesis, it is simple to compute the SED for an arbitrary nominal stress for each simulated R_0 using the Equation (10).

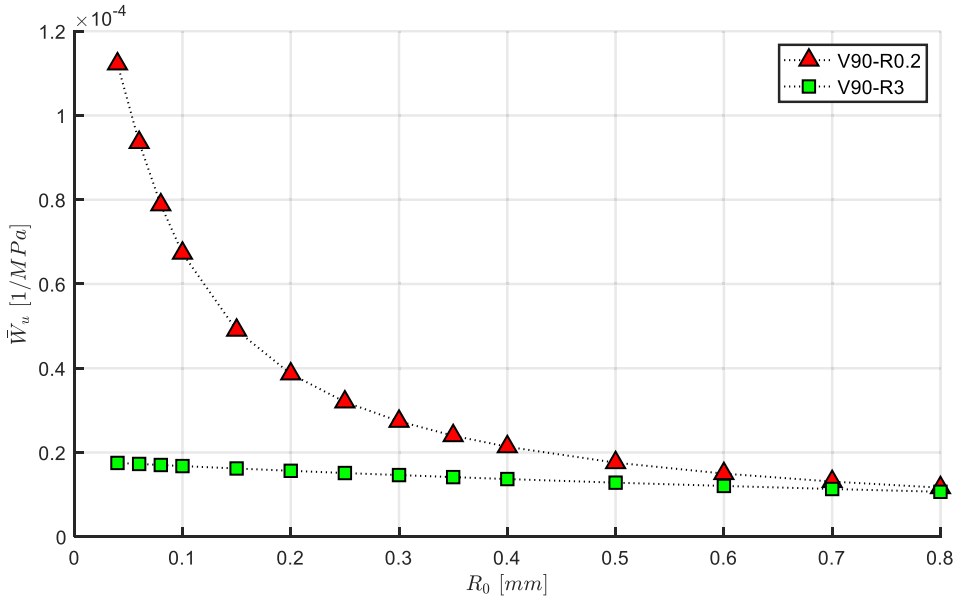

Fig. 9. $\overline{W}_u$. vs R_0 for V90-R0.2 and V90-R3 specimen.

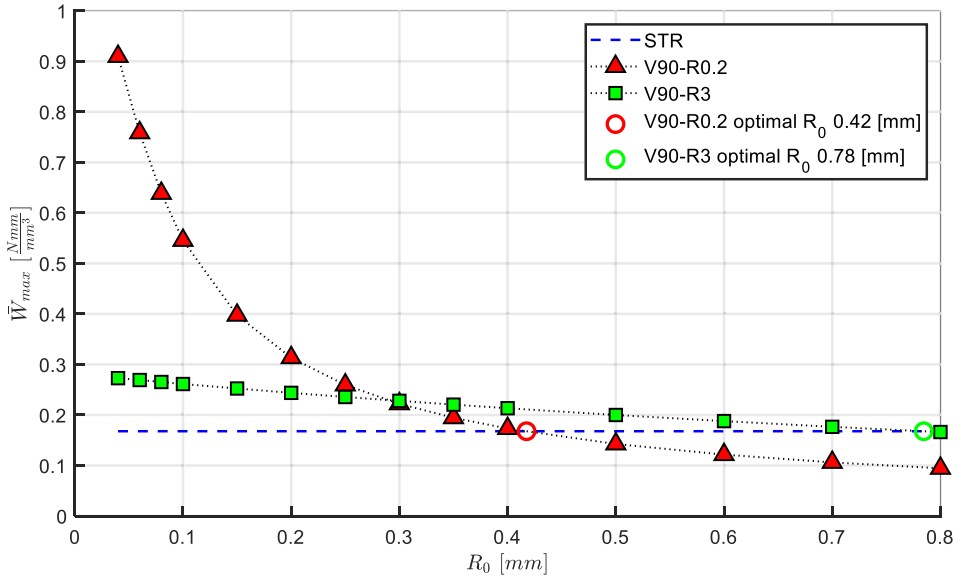

Fig. 10. $\overline{W}$ vs R_0 for V90-R0.2, V90-R3 and STR (smooth) specimens.

$$\Delta\overline{W}_{Exp}^{Notched} = \Delta\overline{W}_u \frac{\left(\Delta\sigma_{Exp}^{Notched}\right)^2}{\left(\Delta\sigma_u\right)^2} \tag{10}$$

To reduce the number of simulations, when the SED value for a critical radius that was not computed by FEA is needed, linear interpolation is used to find the related unitary SED ($\Delta\overline{W}_u$). Following this approach is not only possible to compute the SED value for every R_0 value in the FE analysed range (0.04 to 0.8 mm) but also for every stress level and specimen geometry (Equation (7) and (8)). Practically speaking is now possible to transform the S-N data in form of SED(R_0)-N diagrams. The evaluation of the optimal critical radius is then performed statistically analysing the whole transformed fatigue dataset, finding the R_0 related to the lowest scatter index T_w.

3. Results

3.1. Fatigue properties

Results obtained from the statistical elaboration of fatigue tests data are reported from Figs. 5–7 in form of S-N diagrams. The level of stress is given in absolute values, representing the maximum stress reached by the sinewave. The 50% survival probability curve and the scatter index T_s are calculated for each specimen geometry (excluding validation specimens). Specimens that survived the run-out threshold imposed at 2 million cycles are marked up with a star.

It can be noted that the Wöhler curves show similar scatter index, ranging from 1.176 (V90-R3) to 1.247 (STR). In Fig. 8 all fatigue tests results are presented in a single S-N diagram. From these results, two main observations can be made:

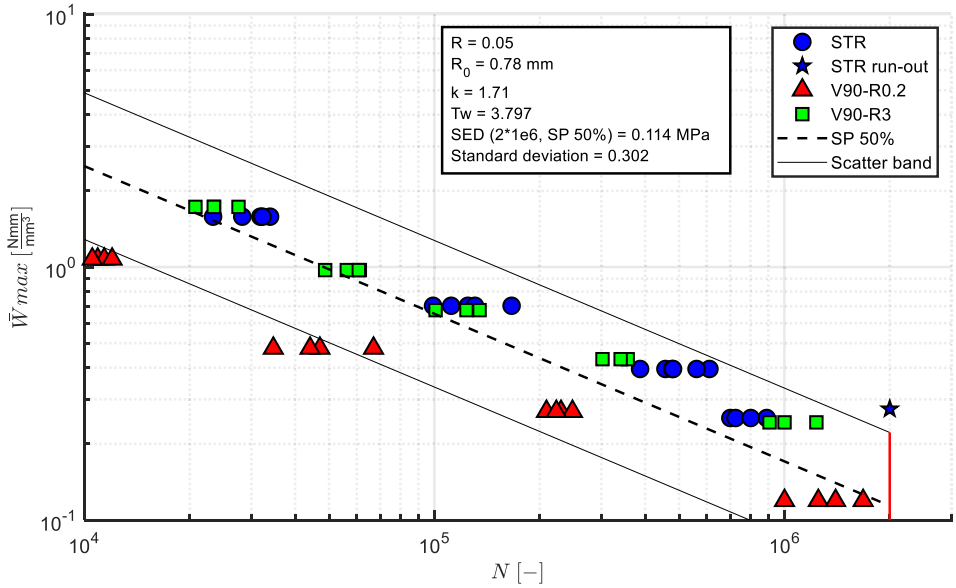

Fig. 11. Fatigue life in terms of $\overline{W}_{max}$ of all R_0 optimization specimens, R_0 obtained equating $\Delta\overline{W}_{Exp}^{V90-R3}$ to $\Delta\overline{W}_{Exp}^{smooth}$.

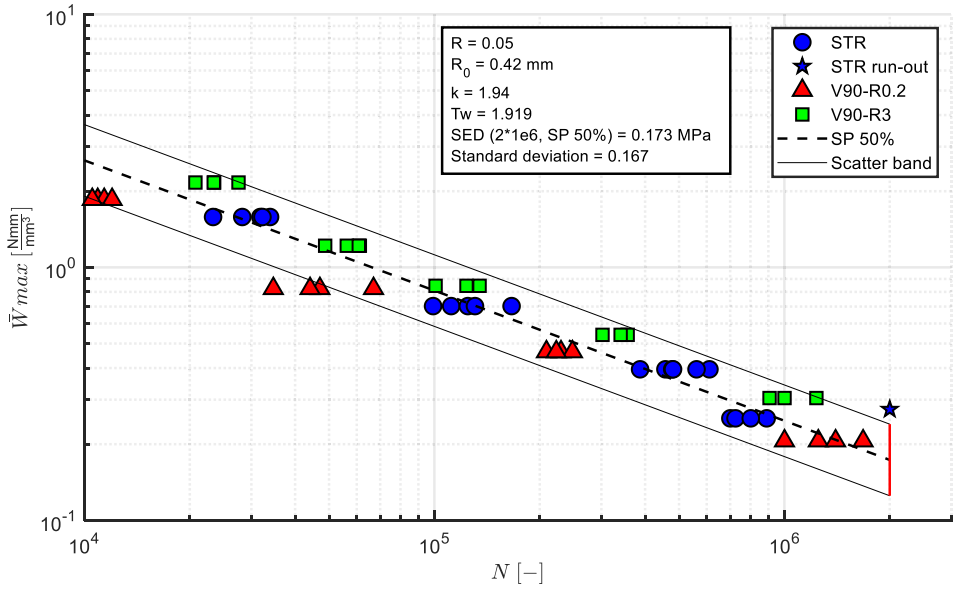

Fig. 12. Fatigue life in terms of $\overline{W}_{max}$ of all R_0 optimization specimens, R_0 obtained equating $\Delta\overline{W}_{Exp}^{V90-R0.2}$ to $\Delta\overline{W}_{Exp}^{smooth}$.

Table 3
R0 value fatigue strength and scatter index for each SED approach.

R_0 selection	R_0 value [mm]	$\Delta\overline{W}_{50\%}$ [a)] [Nmm/mm^3]	Scatter index T_w
Actual approach			
STR –V90-R3 intersection	0.78	0.114	3.797
STR –V90-R0.2 intersection	0.42	0.173	1.919
Proposed approach			
T_w minimization	0.30	0.194	1.692

[a)]Fatigue strength at 2x10^6 cycles.

- Considering the notch stress concentration factor K_t (details in Table 5), the lower the K_t the higher is the fatigue life.
- The notch geometry has a strong influence on the fatigue life of the specimens, with a fatigue life at 2×10^6 cycles which is halved, decreasing from 195 to 90 MPa (details in Table 5) considering the smooth specimen and the sharpest notch tested.

3.2. FEA

Fig. 9 reports FEA results regarding the unitary SED $\Delta\overline{W}_u$ vs R_0. It is possible to notice that the unitary SED raises when the control radius is reduced. Obviously, the unitary SED is higher when the notch stress concentration factor is higher.

As explained in the methods section, the next step is to compute the average SED, $\Delta\overline{W}$ of notched specimen applying the Equation (10) in combination with the $\Delta\overline{W}_u$ and Equation (9) for the STR (smooth) specimen. It is interesting to do this for the fatigue strength of the

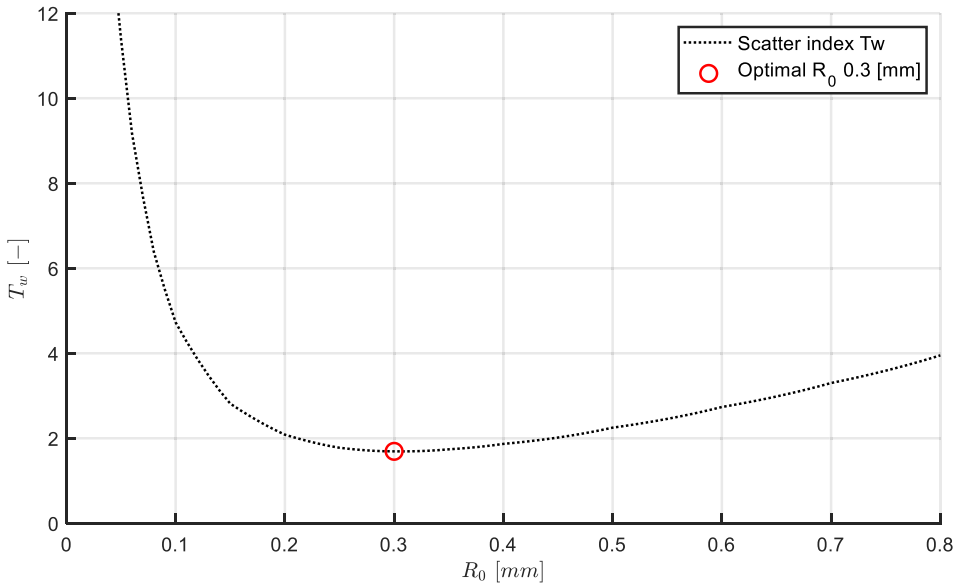

Fig. 13. T_w vs R_0.

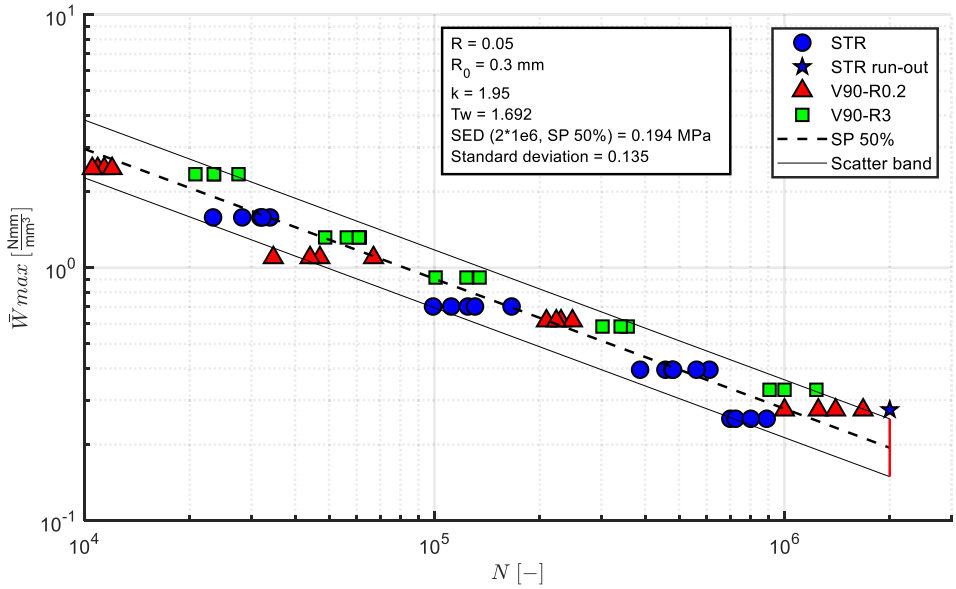

Fig. 14. Fatigue life in terms of $\overline{W}_{max}$ of all R_0 optimization specimens.

specimens at the fatigue limit [23], in this case, the stress related to a survival probability of 50% of the specimen (Table 5)) at 2×10^6 cycles is used. Results are reported in Fig. 10 and is observed that the $\overline{W}_{max}$ curves of the analysed specimen are very close to each other for a critical radius ranging from 0.2 to 0.5 mm. Optimal critical radius is therefore expected to fall inside this range. According to [23] one can obtain the critical radius by varying it until $\Delta\overline{W}_{Exp}^{Notched}$ is equal to $\Delta\overline{W}_{Exp}^{smooth}$. Considering V90-R0.2 specimens the critical radius R_0 turns out to be equal to 0.42 mm, considering V90-R3 specimens 0.78 mm.

SED values of validation specimen are computed by FEA considering directly the optimal R_0.

3.3. Transformed fatigue data – Actual approach

Fatigue data can now be transformed in SED-N curves,Fig. 11 and Fig. 12, adopting the two radiuses found following the actual procedure [23]. Statistical analysis is performed (details can be found in Table 3) and from the graph two observation can be made:

- Critical radius obtained equating $\Delta\overline{W}_{Exp}^{V90-R3}$ to $\Delta\overline{W}_{Exp}^{smooth}$ (0.78 mm) shows a high scatter index T_w of 3.797, with a large number of V90-R0.2 specimens that fall outside the scatter band.
- Critical radius obtained equating $\Delta\overline{W}_{Exp}^{V90-R0.2}$ to $\Delta\overline{W}_{Exp}^{smooth}$ (0.42 mm) shows a much lower scatter index T_w of 1.919. The notch geometry as no more influence on fatigue properties

3.4. Transformed fatigue data – Proposed approach

Following the proposed approach, transformed SED-N fatigue data are statistical analysed and the scatter index T_w is plotted against R_0 in Fig. 13. Following this procedure, the optimal critical radius is found out to be 0.3 mm, and it generates the lower possible scatter index of the transformed dataset, equal to 1.692.

In Fig. 14 is represented the SED-N diagram for the proposed

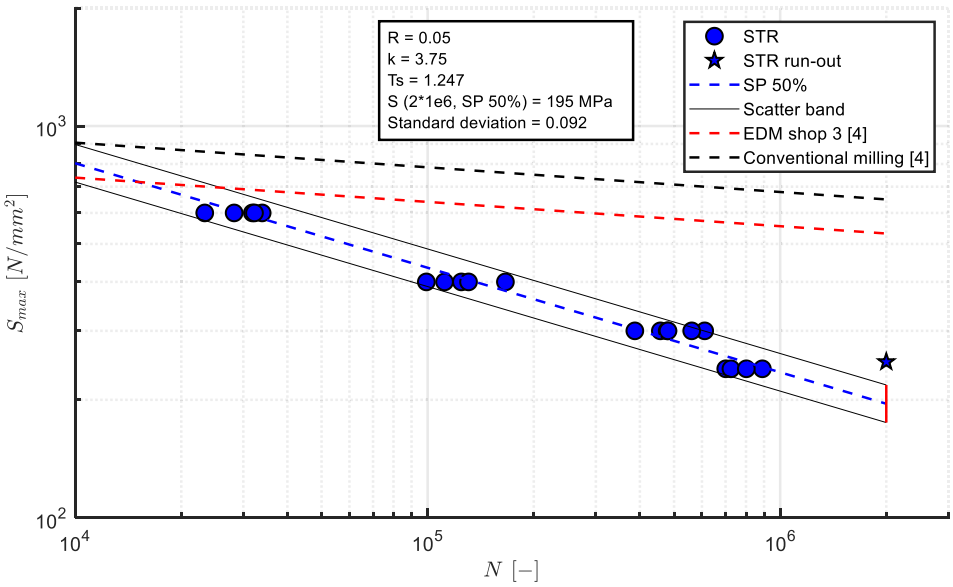

Fig. 15. Fatigue life of un-notched specimen compared to Mower [4].

Table 4
Effect of surface treatment on the fatigue strength of Ti6Al4V [26], modified.

Surface treatment	Methods	Fatigue limit (MPa)[a)]	K_f[b)]
Gentle End mill – peripheral cut [27]	CB[d)], R = -1	455	–
Gentle surface grinding [27]	CB, R = -1	427	0.94
Chemical milling [27]	CB, R = -1	352	0.77
Abusive End mill – peripheral cut [27]	CB, R = -1	220	0.48
Abusive surface grinding [27]	CB, R = -1	90	0.20
Polished (320–600 alumina grit)[28]	RB[e)], R = -1	596	–
Belted and glass bead blasted [28]	RB, R = -1	610	1.02
Belted, beaded, and grit blasted [28]	RB, R = -1	505	0.85
Belted, beaded, shot-peened, and grit blasted [28]	RB, R = -1	555	0.93
Conventional milling [4]	Axial, R = 0.1	649 (at 2×10^6 cycles)	–
WEDM (Shop 3) [4]	Axial, R = 0.1	532 (at 2×10^6 cycles)	0.82[c)]
WEDM (current research)	Axial, R = 0.05	195 (at 2×10^6 cycles)	0.30[c)]

a) At 10^7 cycles.
b) Fatigue strength reduction factor defined as fatigue limit (surface treatment)/fatigue limit (smooth-control) under same testing conditions.
c) Compared to conventional milling [4].
d) Cantilever bending test.
e) Rotating bending test.

Table 5
Fatigue behaviour of the tested specimens.

Specimen name	$\Delta\sigma_{50\%}$[a)] [MPa]	T_σ	k	K_t	$K_{fV-Notch}$	q
STR (smooth)	195	1.247	3.75	1.03	–	–
V90-R0.2	90	1.233	4.46	6.15	2.17	0.23
V90-R3	125	1.176	3.91	1.95	1.56	0.59

a)Fatigue strength at $2x10^6$ cycles.

approach R_0:

- The scatter index T_w is reduced from 1.917 to 1.692;
- The notch geometry has no more influence on the fatigue performance of the specimens, with a fatigue life at 2×10^6 cycles of 0.194 [Nmm/mm^3] in terms of strain energy density;
- Three tests fall outside the uniform 10–90% survival probability scatter band.

4. Discussion

4.1. Fatigue properties

Fatigue properties of Ti6Al4V are severely degraded by the titanium single step technology. Comparing the results obtained with the STR (smooth) specimen with relevant literature [4] the detrimental effect is clear (see Fig. 15). Comparing to conventionally milled specimens [4] (R_a from 1.1 to 1.6 μm) the fatigue strength at 2 million cycles is in fact reduced by a factor of 3. The factor becomes 2.5 considering "EDM shop 3" ones [4]. This reduction can be explained by the strong differences in the surface finish of the two sets of specimens, "EDM shop 3" measured surface roughness R_a ranges from 1.8 to 2.6 μm, considerably lower to the average 3.4 μm roughness of this study dataset. This reduction in the fatigue strength of WEDM specimens can be compensated by use of various chemical or mechanical surface treatment techniques or, partially [4], with the use of a multi step technology. A wide range of surface treatment methods and their influence on the fatigue limit of titanium alloys is provided in Table 4. According to these data, a maximum fatigue limit of around 600 MPa can be achieved for Ti6Al4V using two methods of alumina polishing, and belting and glass bead blasting.

4.2. Notch effect

From Fig. 8 is easy to observe the notch effect on fatigue life. With Equation (11) one can compute the fatigue notch factor $K_{f\,V-Notch}$ and with Equation (12) the notch sensitivity q.

$$K_{f\,V-Notch} = \frac{\Delta\sigma_A^{Smooth}}{\Delta\sigma_A^{V-Notch}} \tag{11}$$

$$q = \frac{K_{f\,V-Notch} - 1}{K_t - 1} \tag{12}$$

Notch stress concentration factor K_t (evaluated on the nominal stress in the reduced section) of notched specimen is evaluated by FEA assuming linear elastic behaviour of the material (refer to Table 2 for FEA material properties).

With the data collected, it is possible to evaluate the notch sensitivity

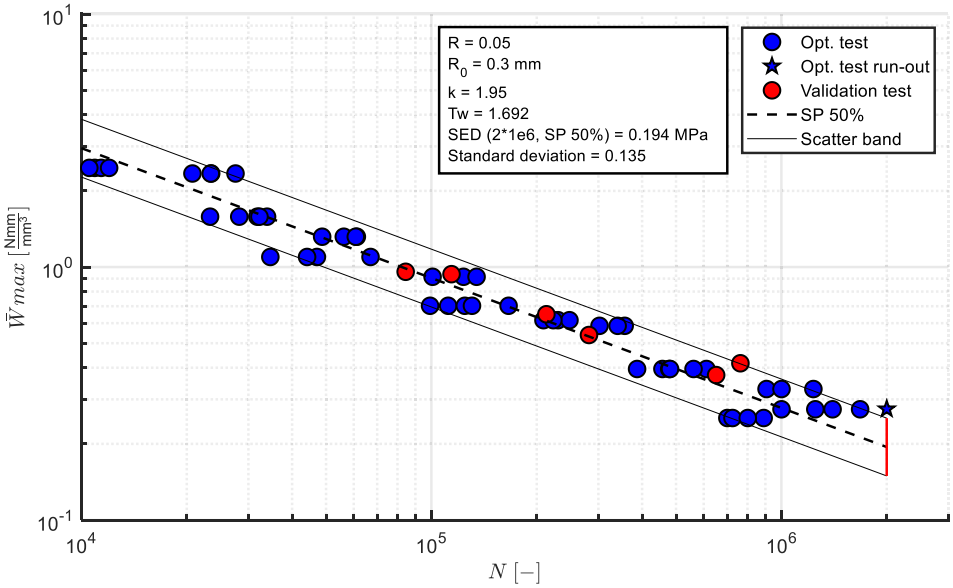

Fig. 16. Fatigue life in terms of $\overline{W}_{max}$ of all specimens.

from two different notch geometries, V90-R3 and V90-R0.2, obtaining a q ranging from 0.59 to 0.23. These values are fairly higher compared to SLM produced specimens with similar K_t value ($K_t = 2.28$, $q = 0.54$) [17]. Looking at Razavi and Berto [18], the notch sensitivity of the V90-R3 specimen is smaller than the wrought machined specimens ($K_t = 2.279$, $q = 0.26$), while similar values were reported for machined specimens fabricated via laser engineer net shaping ($K_t = 2.279$, $q = 0.5$).

4.3. Assessment method validation

The proposed approach is capable to summarize the fatigue data with lower scatter compared to the actual numerical procedure [23]. Scatter index is in fact reduced from 3.797 - 1.919, depending on what notch geometry is considered for the R_0 identification, to 1.692. Furthermore, the proposed approach resolves the issue related to the geometry selection for the R_0 identification, which exists when multiple notch geometries are tested.

The fatigue assessment method is validated by testing two more notch geometries and referring to Fig. 16, one can note that all the validation test data fall inside the uniform scatter bands previously computed (10% and 90% survival probability), therefore it is safe to state that the SED method is applicable to sharp and blunt V-notches with opening angle of 90° for axial fatigue loading.

Moreover, the scatter index T_w can be reconverted in terms of stress in order to perform a proper comparison with nominal stress data, Equation (13).

$$T_s = \sqrt{T_w} = \sqrt{1.692} \cong 1.30 \tag{13}$$

Comparing it with the S-N curves scatter index of each geometry Table 3 it is clear that the scatter of all transformed dataset is similar, suggesting independence from the notch geometry.

5. Conclusion

The fatigue life of Ti6al4V notched and un-notched specimen, machined by WEDM (standard 1 step technology) was successfully assessed by means of SED method following a modified numerical approach. The following conclusion can be drawn from the present work:

- WEDM single step technology has a detrimental effect on the fatigue behaviour of annealed Ti6Al4V, quantifiable with a K_f of 0.3 compared to conventional milling.
- Notch sensitivity is evident, equal to 0.23 for the sharpest notch geometry tested.
- Synthesis of fatigue data was successfully performed by means of the SED method. Fatigue data are then summarized in a single scatter band irrespective of the specimen geometry.
- The proposed numerical approach of the SED method is capable to reduce the scatter index compared to the actual procedure with modest extra effort. Furthermore, it solves the issue related to the geometry selection for the critical radius identification.

Declaration of Competing Interest

The authors declare that they have no known competing financial interests or personal relationships that could have appeared to influence the work reported in this paper.

References

[1] Boyer R, Welsch G, Collings EW. Materials properties handbook : titanium alloys. 1994.
[2] Zahavi E, Torbilo V. Fatigue design: life expectancy of machine parts. Choice Rev Online 1997;34:34-3335-34–3335. 10.5860/CHOICE.34-3335.
[3] Pramanik A, Dixit AR, Chattopadhyaya S, Uddin MS, Dong Yu, Basak AK, et al. Fatigue life of machined components. Adv Manuf 2017;5(1):59–76.
[4] Mower TM. Degradation of titanium 6Al-4V fatigue strength due to electrical discharge machining. Int J Fatigue 2014;64:84–96. https://doi.org/10.1016/j.ijfatigue.2014.02.018.
[5] Janeček M, Nový F, Stráský J, Harcuba P, Wagner L. Fatigue endurance of Ti-6Al-4V alloy with electro-eroded surface for improved bone in-growth. J Mech Behav Biomed Mater 2011;4:417–22. https://doi.org/10.1016/j.jmbbm.2010.12.001.
[6] Klocke F, Welschof L, Herrig T, Klink A. Evaluation of contemporary wire EDM for the manufacture of highly loaded titanium parts for space applications. Procedia Manuf 2018;18:146–51. https://doi.org/10.1016/j.promfg.2018.11.019.
[7] Klocke F, Welling D, Dieckmann J. Comparison of grinding and Wire EDM concerning fatigue strength and surface integrity of machined Ti6Al4V components. Procedia Eng 2011;19:184–9. https://doi.org/10.1016/j.proeng.2011.11.099.
[8] Welling D. Results of surface integrity and fatigue study of wire-EDM compared to broaching and grinding for demanding jet engine components made of Inconel 718. Procedia CIRP 2014;13:339–44. https://doi.org/10.1016/j.procir.2014.04.057.
[9] Lazzarin P, Zambardi R. A finite-volume-energy based approach to predict the static and fatigue behavior of components with sharp V-shaped notches. Int J Fract 2001;112:275–98. https://doi.org/10.1023/A:1013595930617.

[10] Berto F, Lazzarin P. Recent developments in brittle and quasi-brittle failure assessment of engineering materials by means of local approaches. Mater Sci Eng R Reports 2014;75:1–48. https://doi.org/10.1016/j.mser.2013.11.001.
[11] Berto F, Lazzarin P. A review of the volume-based strain energy density approach applied to V-notches and welded structures. Theor Appl Fract Mech 2009;52:183–94. https://doi.org/10.1016/j.tafmec.2009.10.001.
[12] Berto F, Campagnolo A, Lazzarin P. Fatigue strength of severely notched specimens made of Ti-6Al-4V under multiaxial loading. Fatigue Fract Eng Mater Struct 2015;38:503–17. https://doi.org/10.1111/ffe.12272.
[13] Berto F, Lazzarin P. Fatigue strength of Al7075 notched plates based on the local SED averaged over a control volume. Sci China Physics, Mech Astron 2014;57:30–8. https://doi.org/10.1007/s11433-013-5275-2.
[14] Peron M, Javad Razavi SM, Torgersen J, Berto F. Fracture assessment of PEEK under static loading by means of the local strain energy density. Materials (Basel) 2017;10:1–10. https://doi.org/10.3390/ma10121423.
[15] Peron M, Torgersen J, Berto F. Rupture predictions of notched Ti-6Al-4V using local approaches. Materials (Basel) 2018;11(5):663.
[16] Kusch A, Salamina S, Crivelli D, Berto F. Strain energy density as failure criterion for quasi-static uni-axial tensile loading. Frat Ed Integrità Strutt 2021;15:331–49. https://doi.org/10.3221/IGF-ESIS.57.24.
[17] Razavi SMJ, Ferro P, Berto F, Torgersen J. Fatigue strength of blunt V-notched specimens produced by selective laser melting of Ti-6Al-4V. Theor Appl Fract Mech 2018;97:376–84. https://doi.org/10.1016/j.tafmec.2017.06.021.
[18] Razavi SMJ, Berto F. Directed energy deposition versus wrought Ti-6Al-4V: A comparison of microstructure, fatigue behavior, and notch sensitivity. Adv Eng Mater 2019;1900220:1–15. https://doi.org/10.1002/adem.201900220.
[19] Beltrami E. Sulle condizioni di resistenza dei corpi elastici. Nuovo Cim 1885;18:145–55. https://doi.org/10.1007/BF02824697.
[20] Williams ML. Stress singularities resulting from various boundary conditions in angular corners of plates in extension. J Appl Mech 1952;19:526–8. https://doi.org/10.1115/1.4010553.
[21] Lazzarin P, Berto F. Some expressions for the strain energy in a finite volume surrounding the root of blunt V-notches. Int J Fract 2005;135:161–85. https://doi.org/10.1007/s10704-005-3943-6.
[22] Lazzarin P, Filippi S. A generalized stress intensity factor to be applied to rounded V-shaped notches. Int J Solids Struct 2006;43:2461–78. https://doi.org/10.1016/j.ijsolstr.2005.03.007.
[23] Razavi SMJ, Du Plessis A, Berto F. Structural integrity III. Fundam. Laser Powder Bed Fusion Met. Elsevier 2021:395–422. https://doi.org/10.1016/B978-0-12-824090-8.00005-6.
[24] Properties and Selection: Nonferrous Alloys and Special-Purpose Materials. ASM International; 1990. Doi: 10.31399/asm.hb.v02.9781627081627.
[25] Lazzarin P, Berto F, Zappalorto M. Rapid calculations of notch stress intensity factors based on averaged strain energy density from coarse meshes: Theoretical bases and applications. Int J Fatigue 2010;32:1559–67. https://doi.org/10.1016/j.ijfatigue.2010.02.017.
[26] Long M, Rack H. Titanium alloys in total joint replacement—a materials science perspective. Biomaterials 1998;19:1621–39. https://doi.org/10.1016/S0142-9612(97)00146-4.
[27] Boyer HE. Atlas of Fatigue Curves 1985:518.
[28] Eberhardt AW, Kim BS, Rigney ED, Kutner GL, Harte CR. Effects of precoating surface treatments on fatigue of Ti-6Al-4V. J Appl Biomater 1995;6:171–4. https://doi.org/10.1002/jab.770060305.